

ApproxABFT: Approximate Algorithm-Based Fault Tolerance for Neural Network Processing

Xinghua Xue, *Member, IEEE*, Cheng Liu, *Senior Member, IEEE*,
 Feng Min, Tao Luo, *Member, IEEE*, Yinhe Han, *Senior Member, IEEE*

Abstract—With the growing adoption of neural network models in safety-critical applications such as autonomous driving and robotics, reliability has become a critical metric alongside performance and energy efficiency. Algorithm-based fault tolerance (ABFT) strategies, designed atop standard chip architectures, are both cost-effective and adaptable to different architectures, making them particularly attractive. However, traditional ABFT relies on precise error metrics, triggering error recovery procedures even for minor computational deviations. These minor errors often do not impact the accuracy of the neural network model due to the inherent fault tolerance. To address this inefficiency, we propose an approximate ABFT approach, called ApproxABFT, which initiates error recovery only when computational errors are significant. This approach avoids unnecessary recovery procedures, streamlines the error recovery process, and focuses on correcting impactful errors, ultimately enhancing recovery quality. Additionally, ApproxABFT incorporates a fine-grained blocking strategy to smooth error sensitivity across layers within neural network models. Experimental results demonstrate that ApproxABFT reduces the computing overhead by 67.83% and improves the tolerable bit error rate by an order of magnitude on average compared to classical accurate ABFT.

Index Terms—ABFT, fault tolerance, neural network, approximate computing

I. INTRODUCTION

Neural network architectures such as vision transformers (ViTs) [1]–[3] and convolutional neural networks (CNNs) [4]–[6] have shown outstanding performance in main-stream vision tasks, including objection detection and classification, which have attracted a lot of research efforts from both academia and industry, and are increasingly applied in safety-critical applications such as robotics and autonomous driving. It can be envisioned that the trend will continue and reliability will be a critical metric that determines the adoption of neural network models in these applications. While neural networks are usually compute-intensive, improving the neural network reliability with conventional fault-tolerant approaches such as triple modular redundancy (TMR) and recomputing can

Cheng Liu is the corresponding author. Xinghua Xue is with Hangzhou Institute for Advanced Study, University of Chinese Academy of Sciences. Cheng Liu is with the State Key Lab of Processors, Institute of Computing Technology, Chinese Academy of Sciences. Feng Min is with Institute of Computing Technology, Chinese Academy of Sciences. Tao Luo is with Institute of High Performance Computing, A*STAR, Singapore. Yinhe Han is with Hangzhou Institute for Advanced Study, University of Chinese Academy of Sciences and Institute of Computing Technology, Chinese Academy of Sciences. This paper is supported in part by National Key Research and Development Program of China under grant No.(2022YFB3902802) and National Natural Science Foundation of China (NSFC) under grant No.(62174162).

Manuscript received X X, XXX; revised X X, XXX; revised X X, XXX.

incur considerable overhead or require intensive hardware modification [7]–[12].

Different from the above approaches, algorithm-based fault tolerance (ABFT) [13]–[15] based on checksum consumes much less computing overhead. It typically does not require hardware redesigning and can be applied to different computing architectures. Hence, ABFT has been successfully adopted in many applications with regular computing patterns such as GEMMs, FFT, and CNNs for both higher reliability and less computing overhead. However, the kernel of these different ABFT implementations all rely on accurate checksum-based comparison. Basically, assuming the matrix size is $n \times n$, error detection mainly requires a vector dot product and incurs n MACs while error recovery is more expensive and it requires two matrix-vector multiplication with $2 \times n^2$ MACs. Error recovery will be frequently invoked when there are many computing errors at higher error rate. On the other hand, when there are multiple errors in the same row and column at higher bit error rate, the fault tolerance capability of ABFT is limited and ABFT fails. As a result, the ABFT computing overhead can increase dramatically without effective error recovery at higher error rate.

We notice that neural networks are usually resilient to soft errors and can tolerate many minor computing errors as shown in Section II. With this observation, we propose an approximate ABFT approach, namely ApproxABFT, to leverage the inherent fault tolerance of neural networks and relax the error detection and error recovery metrics in classical ABFT. This enables many minor computing errors can be ignored to avoid expensive error recovery procedures without compromising the model accuracy. At the same time, it enables error recovery to focus on more significant errors. To facilitate the seamless integration of ApproxABFT with various neural network models, including ViTs and CNNs, we utilize general matrix-matrix multiplication (GEMM) as the core computation engine. In this case, we can focus on the implementation of ApproxABFT on GEMM instead. Moreover, we also apply a blocking strategy to split the GEMMs in the model into smaller sub GEMMs. With approximate blocking setups, the block-wise ApproxABFT can achieve higher accuracy with less computing overhead. However, it remains a challenging problem to determine the thresholds required for the large number of GEMMs with different sizes in each neural network model.

Given the diverse accuracy demands of applications and the varying sensitivity of neural network layers to soft errors, it will be inefficient to utilize a fixed threshold across different

scenarios from the perspective of both accuracy and computing overhead. In addition, since different design parameters are interrelated, it is difficult to achieve the optimal design goal when all layers use the same parameter values. Therefore, to address the threshold optimization of ApproxABFT, we customize a multi-parameter collaborative optimization algorithm according to the task goal to find the optimal error detection approximation threshold, error recovery approximation threshold and block size parameters of each layer to coordinate the approximation intensity, ABFT overhead and accuracy, and simultaneously adapts to the error sensitivity variation across the different layers of each neural network. According to our experiments, the resulting ApproxABFT implementation shows clear model accuracy improvement and reduces the fault-tolerant design overhead substantially compared to the accurate ABFT. The contributions of this work are summarized as follows.

- We propose an approximate ABFT (ApproxABFT) to relax the error detection and error recovery in classical accurate ABFT such that expensive error recovery can be reduced and some of the uncorrectable computing errors can be approximated with less accuracy penalty.
- We investigated the fault tolerance of neural networks and analyzed the computing deviation distribution induced by soft errors. We observe that most of the soft error induced deviations of matrix sum and row/column sum are small and pose substantial design space for the proposed ApproxABFT.
- We formulate the threshold optimization problem and propose a multi-parameter collaborative optimization algorithm to address the complex design trade-offs among approximation intensity, fault-tolerant design overhead, and model accuracy.
- According to our experiments, the optimized ApproxABFT implementation reduces the computing overhead by 67.83% and improves the tolerable bit error rate by an order of magnitude on average compared to a classical accurate ABFT.

II. OBSERVATION AND MOTIVATION

In this section, we explore the correlation between computing errors and model accuracy in presence of soft errors which are usually modeled with random bit-flip errors. Then, we brief challenges of using classical accurate ABFT protection against the soft errors.

We take VGG19 on CIFAR10 as an example. We utilize bit error rate (BER) to represent the bit flip error intensity and conduct the reliability analysis based on an operation-wise fault injection platform which injects random bit flip errors to outputs of the primitive operations such as addition and multiplication [16]. Then, we compare the accuracy with the different computing error metrics of the model. Specifically, we utilize output matrix sum deviation (MSD) and row/column sum deviation (R/CSD) to characterize the bit flip errors induced computing deviations.

The comparison in Fig.1(a) reveals the correlation between MSD and model accuracy. Fig.1(b) reveals the correlation

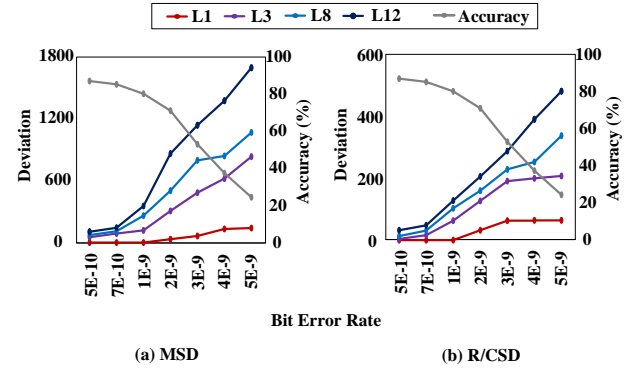


Fig. 1. Correlation between accuracy and computing deviation of matrix sum and row/column sum i.e. MSD and R/CSD.

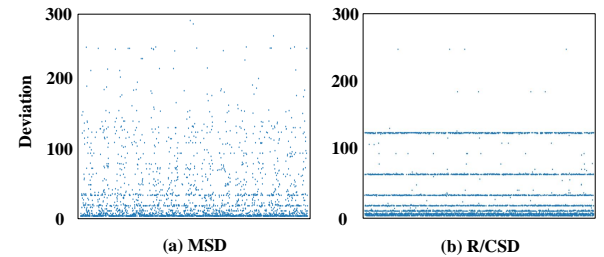


Fig. 2. MSD and R/CSD of the largest output matrix in each VGG19 layer when BER is 7E-10.

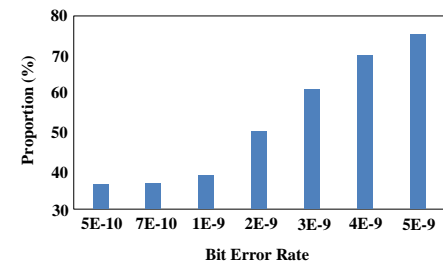


Fig. 3. The percentage of rows and columns that cannot be recovered by ABFT due to multiple computing errors in VGG19.

between R/CSD and model accuracy. L1, L3, L8 and L12 denote the first, third, eighth and twelfth layers in the model, respectively. In general, MSD, R/CSD, and the model accuracy are roughly monolithic to BER and exhibit consistent trend in general despite the distinct values. Thereby, we can leverage MSD or R/CSD as indicators to predict the model accuracy.

To gain insight of the different computing deviations, we set BER to be 7E-10 and present the statistic of MSD and R/CSD of the largest output matrix in each VGG19 layer. The result as shown in Fig.2 demonstrates that the majority of the MSD is close to zero and pose negligible influence on the model accuracy according to the correlation between accuracy and MSD. Similar to MSD, the majority of R/CSD and R/CSD is smaller than 100, which poses little influence on the model accuracy according to Fig.1.

As mentioned, ABFT has limited fault tolerance capability

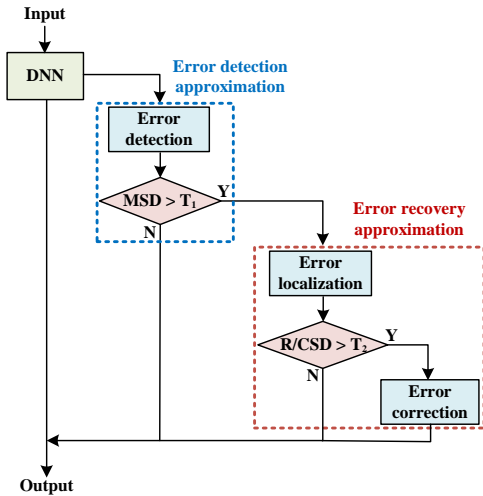


Fig. 4. The architecture of ApproxABFT.

and cannot recover GEMMs with multiple computing errors in the same row and column. The percentage of rows and columns with multiple computing errors that cannot be recovered in VGG19 is presented in Fig.3. It demonstrates that the percentage of computing errors that cannot be recovered with ABFT grows rapidly with the increase of BER. If the recovery procedures are not handled appropriately, classical accurate ABFT will incur substantial computing overhead while contributing little to the model accuracy.

With the above observations, we propose to approximate the algorithm by raising the error thresholds such that smaller computing errors in ABFT can be ignored. The approximation can not only reduce the error recovery overhead but also force the algorithm to focus only on larger computing errors, which essentially improves the probability of successful ABFT error recovery and can be beneficial to the resulting model accuracy.

III. APPROXIMATE ABFT

In this section, we propose an approximate ABFT approach, namely ApproxABFT, which relaxes the error detection and error recovery metrics in the classical accurate ABFT method. It only focuses on and recovers some critical computing errors. Since the fault tolerance capability may vary across different models and different layers in the same model, we further investigate how to approximate ABFT to fully utilize model fault tolerance and reduce the ABFT computing overhead and accuracy loss.

A. ApproxABFT Overview

As shown in Section II, we notice that neural networks are usually resilient to soft errors and can tolerate many minor computing errors. With this observation, we propose ApproxABFT approach, as shown in Fig.4.

In the error detection approximation stage, unlike the classical accurate ABFT method that will invoke error recovery

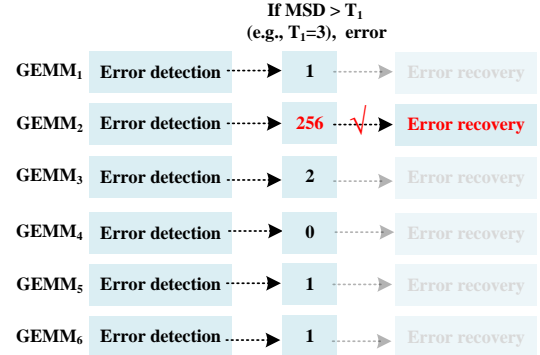


Fig. 5. Error detection approximation.

procedures even if minor computing errors are detected, ApproxABFT selectively invoke the error recovery procedures based on MSD obtained in error detection. Specifically, ApproxABFT relaxes the error standard and ignores computing errors that are smaller than a predefined threshold T_1 , which greatly reduces the number of detected output matrix errors and requires much less error recovery to reduce the overall error tolerance overhead according to the deviation distribution of MSD in Fig.2 in Section II.

For the error recovery approximation stage, we also raise the R/CSD thresholds utilized to locate the computing errors in output matrix. With higher R/CSD thresholds T_2 , minor row/column deviations will be ignored and the number of computing errors to be corrected will be reduced, which can simplify the error correction. Model accuracy can be improved by approximately converting a portion of the uncorrectable case of multiple errors in a row/column into the correctable case of a single error in a row/column.

When the error location is determined, for only one error in a row/column, computing errors will be corrected by adding the computing deviation to the error value at the located location. For multiple errors in a row/column, which cannot be corrected directly after approximation, we further explore how to handle the computing errors to alleviate their influence on model accuracy.

B. Error Detection Approximation

The GEMM operation is expressed as $Y = W \cdot X$, where W is the weight matrix, X is the input matrix, and Y is the output matrix. When performing error detection approximation, the deviation value MSD between the predicted matrix checksum C_L and the output matrix checksum C_R is calculated, as shown in Equation1. Assume that the matrix dimension is N , α is an N -dimensional vector $[1, 1, \dots, 1]$. When $MSD > T_1$, it indicates that there is a non-negligible computing error and the error recovery process needs to be invoked. When $MSD \leq T_1$, it indicates that the impact of the computing error on the result is negligible, and the subsequent expensive error recovery calculation is skipped, as shown in Equation2.

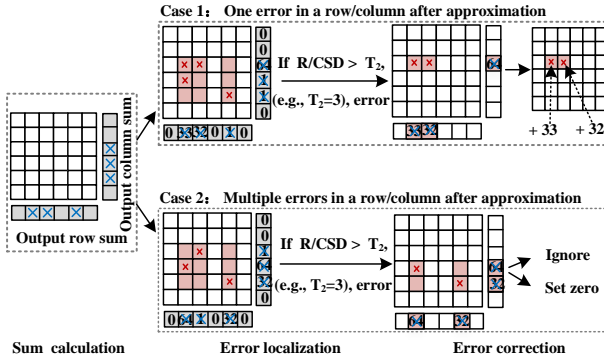


Fig. 6. Error recovery approximation.

$$\begin{aligned}
 C_L &= \alpha W \cdot X \alpha^T, \\
 C_R &= \sum_{i=1}^N \sum_{j=1}^N Y_{ij}, \\
 MSD &= |C_L - C_R|, \\
 \begin{cases} \text{Invoke error recovery} & \text{if } MSD > T_1 \\ \text{Skip} & \text{if } MSD \leq T_1 \end{cases} & (2)
 \end{aligned}$$

By raising the error detection threshold T_1 , we can avoid recovering many minor computing errors that pose little influence on the model accuracy and reduce the computing overhead accordingly. Fig.5 shows an example of error detection approximation for six GEMM operations. Assuming that the approximation threshold is increased from nearly 0 in classical accurate ABFT to 3 in ApproxABFT, the number of expensive error recovery processes that need to be invoked decreases from 5 to 1, resulting in a significant reduction in fault tolerance overhead.

C. Error Recovery Approximation

The error recovery approximation stage can be split into sum calculation, error localization, and error correction. Sum calculation remains unchanged for different error recovery strategies, as shown in Equation3. we mainly investigate how error localization and error correction can be approximated in this sub section.

$$\begin{aligned}
 C_{L_Row} &= \alpha W \cdot X, \\
 C_{R_Row} &= \sum_{i=1}^N Y_i, \\
 C_{L_Col} &= W \cdot X \alpha^T, \\
 C_{R_Col} &= \sum_{j=1}^N Y_j, \\
 R/CSD &= [|C_{L_Row} - C_{R_Row}|, |C_{L_Col} - C_{R_Col}|]
 \end{aligned} \quad (3)$$

Error localization essentially utilizes R/CSD to validate computing results in each row and each column of the output matrix. With both the error row ID and column ID, we can

determine the possible faulty elements of the output matrix as shown in Fig.6. Usually, more elements need to be corrected when there are more faulty rows and columns. Thus, we also raise the threshold T_2 of the error metric of R/CSD such that only significant computing errors are identified. By skipping minor computing errors, it turns some of the uncorrectable errors to be correctable ones and enhances the model accuracy eventually.

As for the error correction approximation, it can be divided into two different occasions. In the first occasion, computing errors in the output matrix can be perfectly corrected by adding the corresponding R/CSD to the faulty element when there is only one possible faulty element in a row or in a column after approximation. In the second occasion, we cannot recover the faulty elements with only R/CSD when there are more than one possible faulty elements in the corresponding rows and columns after approximation. In this case, we approximate the correction by resetting the possible faulty elements to alleviate the negative influence. A straightforward approach is to ignore faulty elements, however, these computing errors can have a negative influence on the model accuracy. To this end, we approximate the correction by resetting the possible faulty elements to zero and cut the error propagation.

D. ApproxABFT Blocking

In order to further optimize the error recovery capability when a GEMM is large and multiple errors may happen at the same time, we further propose a block-wise ApproxABFT method. To this end, we divide large GEMMs into sub GEMMs blocks and apply ApproxABFT on sub GEMMs, which can also smooth the threshold variations across GEMMs with distinct sizes. As for the block size setups, the blocking will induce more detection overhead but potentially reduce the recovery overhead and improve the recovery quality because of the fine-grained fault-tolerant processing. Specifically, we start the error detection based on the overall GEMM. If the GEMM turns out to be fault-free, we can skip the error recovery. If faults are detected, we will further start the block-wise error detection and error recovery. Hence, the computing overhead of the block-wise ApproxABFT consists of error detection of the entire GEMM, error detection of all the sub GEMMs, and error recovery of the faulty sub GEMMs. Since we focus on the ABFT overhead in this stage, optimized blocking setup is affected by the bit error rate and can be determined, while ApproxABFT is applied on top of the blocking.

E. Multi-parameter Collaborative Optimization

Since the sizes and fault sensitivities of different layers vary greatly, and different design parameters are interrelated, it is difficult to achieve the optimal design goal when all layers use the same parameter values. Therefore, in order to achieve a better trade-off between fault tolerance accuracy and redundant protection overhead, it is necessary to construct a multi-parameter collaborative optimization algorithm to achieve the optimal fault tolerance design by finding the optimal error detection approximation threshold, error recovery approximation threshold, and block size parameter for each layer. However,

due to the large parameter design space, manual optimization is difficult to fulfill complex design goals and has low design efficiency. To solve the parameter optimization problem, we use the Bayesian optimization algorithm as the base and then customize it for our task. The accuracy requirement of the model under a specified bit error rate is used as a design constraint to minimize the fault tolerance overhead. By searching for the optimal parameter combination, the fault tolerance performance can be automatically adjusted. The design space exploration problem is formalized as Equation 4.

$$\begin{aligned} & \text{argmin } \text{overhead}, \\ & \text{s.t. } acc \geq \text{Specified target accuracy} \end{aligned} \quad (4)$$

The multi-parameter collaborative optimization algorithm is shown in Algorithm 1. We first create a Bayesian optimizer and initialize the sample set. Generate a given set of observations in the search space (Line 3-7). Then use the Bayesian to obtain the posterior distribution, and the acquisition function instructs Bayesian to select the next search point (Line 8). Under the guidance of the posterior distribution and the acquisition function, Bayesian searches for t points (Line 9-14). Finally, return to the optimal parameter configuration (Line 15).

Algorithm 1 Multi-parameter collaborative optimization algorithm

Input: Randomly generate n sets of parameter configurations to initialize the design parameter space S , the number of times to find the optimal solution t .

Output: Optimized parameter selection p .

```

1: Bayes_Opt()                                ▷ Create Bayesian Optimizer
2:  $P \leftarrow \emptyset$                           ▷ Initialize the sample set
3: for  $i = 1, \dots, n$  do
4:    $s \leftarrow S_n$                             ▷ Get parameter configuration
5:    $acc, overhead \leftarrow Get\_FT\_Val(s)$  ▷ Get the fault tolerance
   accuracy and overhead under the current parameter configuration
6:    $P.append(s, acc, overhead)$                 ▷ Add new sample to P
7: end for
8: Bayes_Opt.optimize(P)                  ▷ Estimate posterior distribution and
   acquisition function
9: for  $i = 1, \dots, t$  do
10:   $s \leftarrow Bayes\_opt.select\_next\_sample()$ 
11:   $acc, overhead \leftarrow Get\_FT\_Val(s)$ 
12:   $P.append(s, acc, overhead)$ 
13:  Bayes_Opt.optimize(P)                  ▷ Bayesian optimization to tune
   parameters
14: end for
15: return the optimized parameter selection point  $p$ 

```

IV. EXPERIMENT RESULTS

A. Experimental Setup

We select four models including VGG19 [17] on CIFAR10 dataset [18], ResNet101 [19], DeepViT-S [20] and CaiT-XXS-24 [21] on ImageNet-1K dataset [22] as the benchmark. We utilize bit error rate (BER) to represent the error intensity and conduct the reliability analysis based on an operation-wise fault injection platform which injects random bit flip errors to outputs of the primitive operations such as addition and multiplication [16]. The different ABFT setups are summarized in Table I. For the error detection, we implemented both baseline detection (BED) and approximate detection (AED).

Similarly, we implemented baseline error localization (BEL) and approximate error localization (AEL). The baseline error correction (BEC) ignores the computing errors that cannot be recovered while approximate error correction (AEC) sets the uncorrectable elements in the output matrix to be zero. All the experiments are performed on a server equipped with two 24-core@2.5GHz Intel Xeon processors, 512GB memory, and four PH402 SKU200 GPU cards.

TABLE I
SETUPS AND NOTATIONS OF DIFFERENT ABFT IMPLEMENTATIONS

	Error Detection	Error Recovery		Block
		Error Localization	Error Correction	
AccurateABFT [23]–[28]	BED	BEL	BEC	✗
Block-AccurateABFT [29]	BED	BEL	BEC	✓
ApproxABFT	AED	AEL	AEC	✗
Block-ApproxABFT	AED	AEL	AEC	✓

B. Overall Fault-tolerant Design Evaluation

To demonstrate the performance advantage of the proposed approximate ABFT fault-tolerant design, we evaluate different ABFT fault-tolerant methods from the perspective of model Top-1 accuracy and computing overhead under various BER setups. The detailed setup of the different ABFT fault-tolerant methods is summarized in Table I.

1) **ApproxABFT:** The proposed ApproxABFT is compared with the state-of-the-art AccurateABFT fault-tolerant method [23]–[28]. The accuracy comparison is presented in Fig.7(a). In general, AccurateABFT mainly benefits at lower BER when the number of computing errors is small and the errors can be recovered. In contrast, ApproxABFT greatly extends the BER range that can be protected by an order of magnitude. The overhead comparison is presented in Fig.7(b). Computing overhead is normalized to that of AccurateABFT. Compared with the AccurateABFT, ApproxABFT generally reduced the computing overhead by an average of 43.39%, which is mainly attributed to the error detection approximation that reduces considerable error recovery procedures. At the same time, we notice that the number of addition and multiplication operations required by ApproxABFT also reduces considerably, which also confirms the computing overhead benefits of ApproxABFT.

2) **Block-ApproxABFT:** Since blocking essentially changes the granularity of ABFT and can be integrated with ApproxABFT, we further compare the proposed Block-ApproxABFT with AccurateABFT, ApproxABFT, and the state-of-the-art Block-AccurateABFT fault-tolerant method [29]. As shown in Fig.7, blocking is an effective approach to enhance ABFT. Block-ApproxABFT achieves higher model accuracy and requires less computing overhead at all different BER setups. Compared to AccurateABFT, ApproxABFT, Block-AccurateABFT fault-tolerant method, Block-ApproxABFT reduced the average by 67.83%, 36.67%, and 12.35% respectively. The main reasons can be attributed to two aspects. On the one hand, the larger GEMM is divided into multiple sub-blocks, and the random bit flip errors are scattered in different sub-blocks, the number of errors in a single sub-block

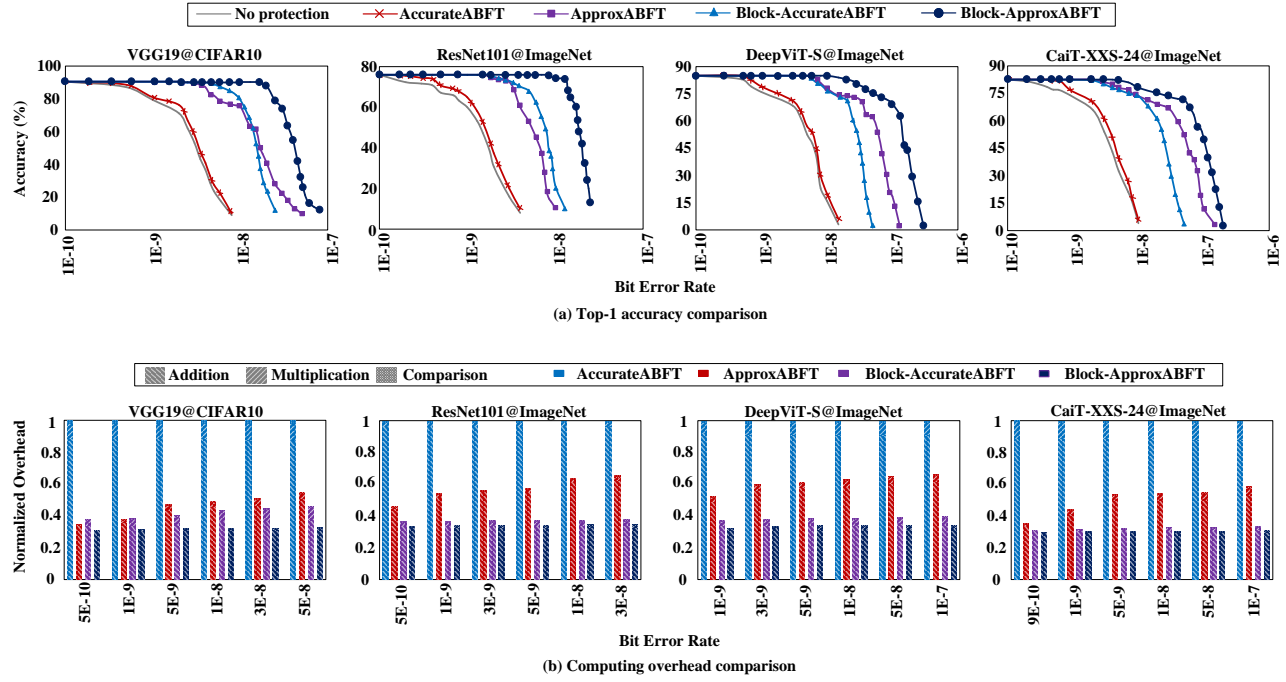


Fig. 7. Accuracy and computing overhead comparison between ApproxABFT, Block-ApproxABFT, AccurateABFT [23]–[28], and Block-AccurateABFT [29].

is significantly reduced, which greatly improves the success rate of error recovery. On the other hand, some sub-blocks are fault-free, and only the faulty sub-blocks are approximated, which can reduce the total computing overhead.

C. ApproxABFT Different Approximate Strategies Evaluation

To gain insight of ApproxABFT, we have the approximation of error detection (AED), error localization (AEL), error correction (AEC) applied progressively and evaluate the model accuracy and computing overhead respectively.

1) **AED:** As presented in Fig.8, AED does not affect the model accuracy but it contributes most to the overall computing overhead. This is mainly because that it skips many trivial computing errors in error detection as demonstrated in Fig.9(a). Although the percentage of the skipped computing errors decreases with growing BER, the number of skipped computing errors remains non-trivial, which leads to less error recovery.

2) **AEL:** Different from AED, AEL pose little influence on the computing overhead, but AEL shows clear model accuracy improvement under various BER setups mainly because it skips minor computing errors making it possible for ApproxABFT to correct the more significant computing errors. The experiment in Fig.9(b) demonstrates the increased correctable computing errors. However, the benefits can be limited when the number of significant computing errors exceeds the fault tolerance capability of ABFT.

3) **AEC:** AEC demonstrate a negligible influence in computing overhead, but they play a key role in model accuracy improvement. Unlike AEL, AEC is particularly effective when BER is high and there are many uncorrectable computing errors. Basically, setting the computing errors to be zero poses

less negative influence on the model accuracy because it is more like a random dropout, which is also verified in prior works [30].

D. Approximation Parameter Analysis

In this sub section, we explore the influence of the different design parameters on the model accuracy and computing overhead in the approximate ABFT.

1) **Different MSD Threshold Analysis:** Thresholds are critical to the proposed ApproxABFT algorithm. We compared our proposed optimization threshold strategy with the strategy of setting all GEMMs in the model to a fixed threshold, and explored the impact of different T_{MSD} thresholds. Fig.10 illustrates the impact of varying T_{MSD} thresholds setting on both model accuracy and computing overhead. There are three different fixed threshold settings. We noticed that the optimized strategy shows significant advantages in both accuracy and computing overhead compared to the fixed threshold setting. Moreover, as the T_{MSD} threshold increases, both model accuracy and fault-tolerant computing overhead decrease. This trend primarily stems from more error recovery processes can be filtered out, thereby reducing computing overhead, but has more negative impact on model accuracy.

2) **Different R/CSD Threshold Analysis:** Fig.11 shows the impact of different $T_{R/CSD}$ thresholds setting strategies on model accuracy and computing overhead. Similarly, there are three different fixed $T_{R/CSD}$ threshold settings, and then they were compared with the proposed optimization threshold strategy. It can be seen that different thresholds result in different accuracy gains, but the impact of computing overhead is negligible. The advantages of the optimized threshold is particularly significant at higher error rate when multiple faulty

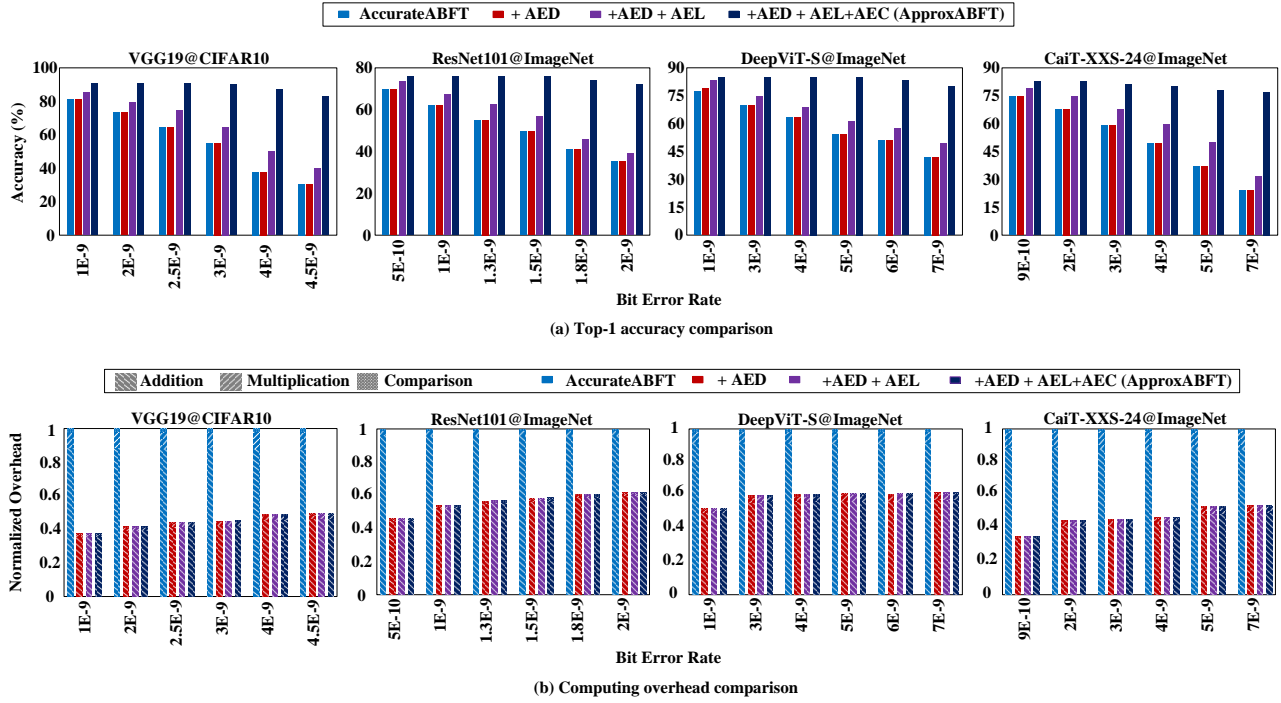


Fig. 8. Top-1 accuracy and computing overhead evaluation of the different approximation strategies including AED, AEL, and AEC.

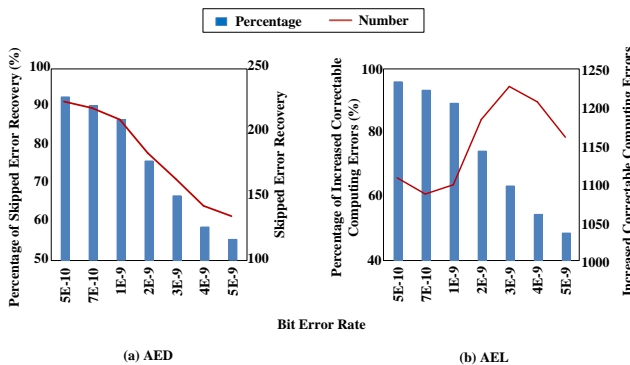


Fig. 9. (a) percentage of the skipped error recovery brought by AED over the total error recovery of AccurateABFT. (b) percentage of increased correctable computing errors brought by AEL over the total number of uncorrectable computing errors of AccurateABFT.

elements may occur in the same GEMM output and the number of the errors to be recovered can be reduced by the error localization approximation.

3) **Different Block Size Analysis:** As demonstrated in IV-B, Block-ApproxABFT shows significant advantages over the non-blocking ApproxABFT in terms of both model accuracy and computing overhead. We further investigate the influence of block size setups on Block-ApproxABFT. Suppose all the blocks are square and it is utilized across all the different GEMMs in model. The size of the square matrix ranges from 16 to 64. We have them implemented and compared with the optimized blocking. The comparison is presented in Fig.12. It can be seen that smaller block sizes achieve

higher model accuracy in general because of the more fine-grained error detection and recovery granularity. Although the optimized block size setting is less accurate than the fixed 16 block size setting in some high error rate scenarios, it is significantly less expensive in terms of overhead at different error rates. As for the computing overhead, optimized block size can neither be too small or too large because small blocks will induce considerable error detection overhead while large blocks can result in frequent failed error recovery procedures. However, fixed block size setups fail to adapt the GEMMs with different sizes and the proposed optimized partitioning is mostly outperforms the fixed setups on computing overhead.

V. RELATED WORK

General matrix-matrix multiplication (GEMM) plays an important role in the calculation of neural networks. The major computing kernels in ViTs such as multi-head attention and feed forward are usually implemented with GEMM, and the convolution operation of CNN can also be realized by an efficient conversion strategy to GEMM operation [31]. ABFT [13] originally developed for resilient GEMMs becomes a promising approach for fault-tolerant neural network models accordingly. ABFT induced computing patterns are generally consistent with GEMMs and the computing overhead is much less compared to classical redundancy-based approaches. Hence, it has been explored intensively for fault-tolerant design of many regular tensor-based operations, such as FFT [32], [33], sparse operations [34], [35], decomposition [36]–[39], sorting [40], [41].

Recently, it has also been intensively explored for protecting neural network models against soft errors on various

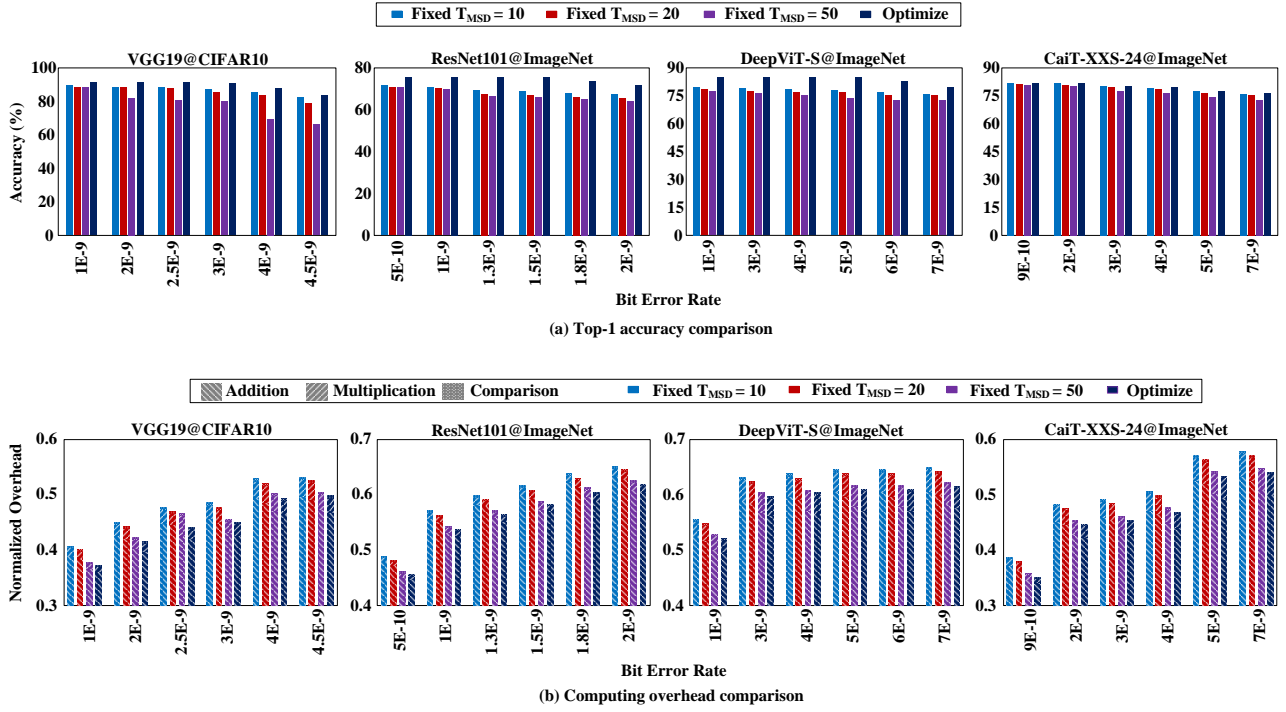


Fig. 10. Influence of different MSD threshold setups on ApproxABFT. Normalized computing overhead is relative to AccurateABFT overhead.

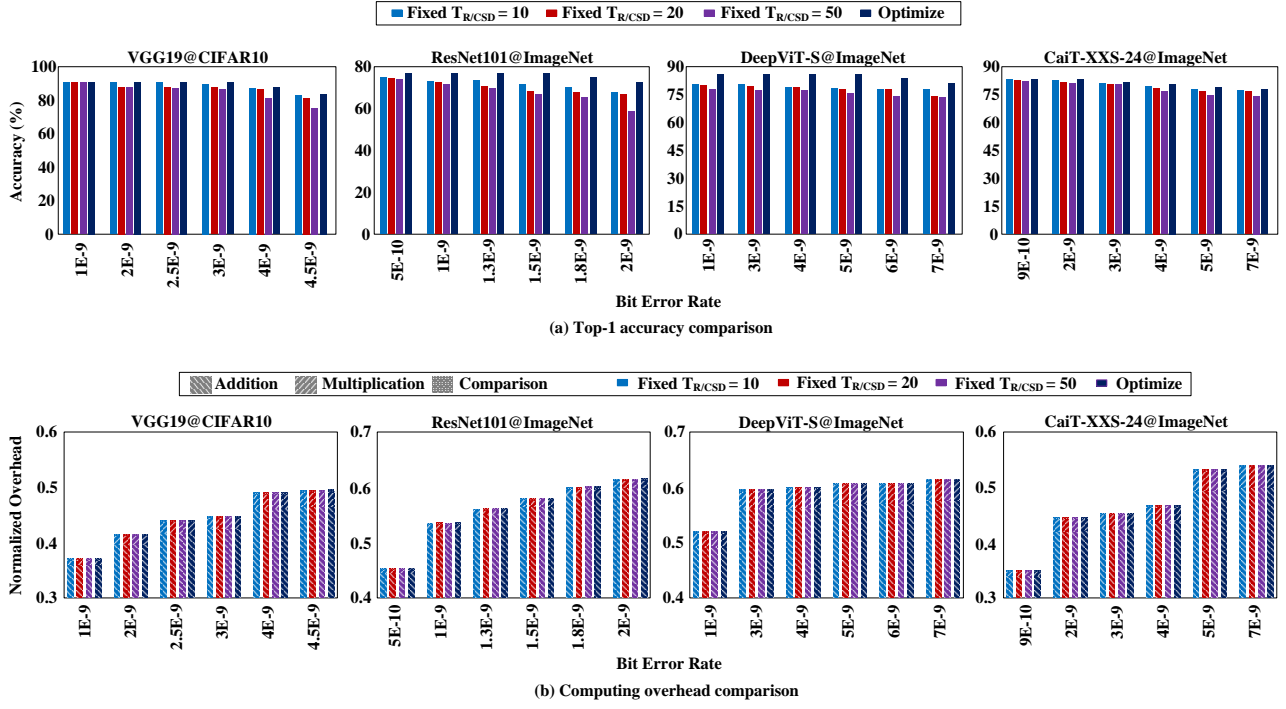


Fig. 11. Influence of different R/CSD threshold setups on ApproxABFT. Normalized computing overhead is relative to AccurateABFT overhead.

computing engines [42]–[46]. For instance, [42] proposed four ABFT schemes including full checksum, column checksum, row checksum and checksum-of-checksum to protect the convolutional layers of different parameters against soft errors, and designed a multi-scheme workflow to obtain high

detection/correction capability with less runtime overhead. [43] leveraged the high compute-to-memory-bandwidth ratios of GPUs to reduce the execution-time overhead significantly. [44] presented a design of a high-performance GPU-based GEMM that integrated an algorithm-based fault tolerance

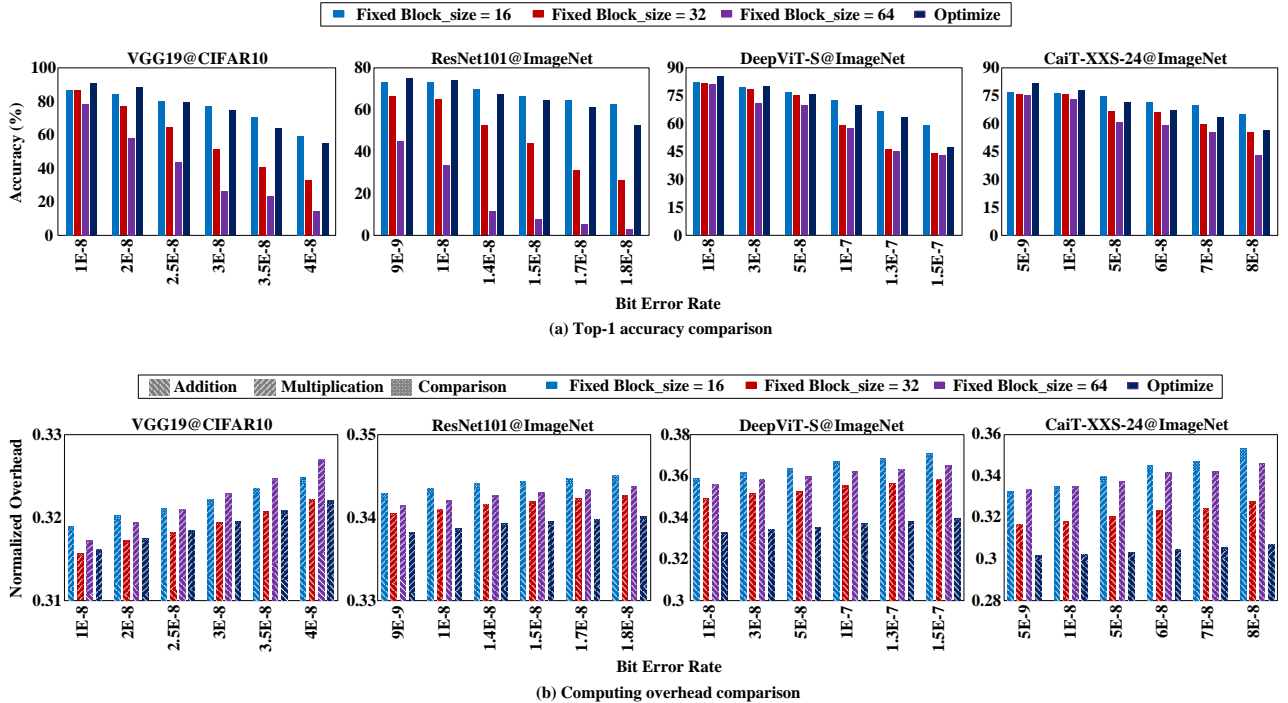


Fig. 12. Influence of block size setups on Block-ApproxABFT. Normalized computing overhead is relative to AccurateABFT overhead.

scheme and explored fused ABFT schemes for GEMM with respect to the thread level, warp level, and threadblock level. [45] conducted the comprehensive fault injection and error propagation study on the attention mechanism against INF, NaN, and near-INF errors, and designed a highly optimized ABFT for these faults, including propagating errors, unpredictable patterns, and mixed error types. [46] proposed a high-performance FFT implementation equipped with a two-sided fault tolerance scheme that detects and corrects silent data corruptions at computing units on-the-fly. These different approaches generally follow the accurate checksum mechanism used in classical accurate ABFT and can benefit from the proposed approximate checksum strategy.

VI. CONCLUSION

In this work, we propose an approximate ABFT algorithm, namely ApproxABFT, for the first time. Instead of using strict metrics for error detection and error localization in standard accurate ABFT, ApproxABFT presents a soft error metric by raising the error thresholds with a multi-parameter collaborative optimization algorithm such that the thresholds can filter out minor computing errors, and match the fault tolerance of the different GEMMs in neural network model for the sake of both higher accuracy and lower computing overhead can be taken into consideration in a unified framework. In addition, ApproxABFT also utilizes a simple yet effective error correction (zero-out) approach to handle the uncorrectable computing errors and alleviate the negative influence of these errors on model accuracy. Finally, we also investigate influence of GEMM blocking on ApproxABFT and adapt the block size to suit GEMMs with different sizes across each model. Ac-

cording to our experiments, the proposed ApproxABFT shows significant accuracy improvement and much lower computing overhead compared to classical accurate ABFT. It is a simple yet effective approach and can be potentially applied to protect generic GEMM-based approximate computing tasks against soft errors.

REFERENCES

- [1] L. Papa, P. Russo, I. Amerini, and L. Zhou, "A survey on efficient vision transformers: algorithms, techniques, and performance benchmarking," *IEEE Transactions on Pattern Analysis and Machine Intelligence*, 2024.
- [2] X. Li, H. Ding, H. Yuan, W. Zhang, J. Pang, G. Cheng, K. Chen, Z. Liu, and C. C. Loy, "Transformer-based visual segmentation: A survey," *IEEE Transactions on Pattern Analysis and Machine Intelligence*, 2024.
- [3] J. Zhang, J. Huang, S. Jin, and S. Lu, "Vision-language models for vision tasks: A survey," *IEEE Transactions on Pattern Analysis and Machine Intelligence*, 2024.
- [4] X. Zhao, L. Wang, Y. Zhang, X. Han, M. Deveci, and M. Parmar, "A review of convolutional neural networks in computer vision," *Artificial Intelligence Review*, vol. 57, no. 4, p. 99, 2024.
- [5] A. Younesi, M. Ansari, M. Fazli, A. Ejlali, M. Shafique, and J. Henkel, "A comprehensive survey of convolutions in deep learning: Applications, challenges, and future trends," *IEEE Access*, vol. 12, pp. 41180–41218, 2024.
- [6] H. Issaoui, A. ElAdel, and M. Zaied, "Object detection using convolutional neural networks: A comprehensive review," in *2024 IEEE 27th International Symposium on Real-Time Distributed Computing (ISORC)*, pp. 1–6, IEEE, 2024.
- [7] R. E. Lyons *et al.*, "The use of triple-modular redundancy to improve computer reliability," *IBM journal of research and development*, vol. 6, no. 2, pp. 200–209, 1962.
- [8] S. Liu *et al.*, "Result-based re-computation for error-tolerant classification by a support vector machine," *IEEE Transactions on Artificial Intelligence*, vol. 1, no. 1, pp. 62–73, 2020.
- [9] D. Xu *et al.*, "R2f: A remote retraining framework for aiot processors with computing errors," *IEEE Transactions on Very Large Scale Integration (VLSI) Systems*, vol. 29, no. 11, pp. 1955–1966, 2021.

[10] Q. Zhang, C. Liu, B. Liu, H. Huang, Y. Wang, H. Li, and X. Li, "Cross-layer optimization for fault-tolerant deep learning," *arXiv preprint arXiv:2312.13754*, 2023.

[11] H. Sayadi *et al.*, "A data recomputation approach for reliability improvement of scratchpad memory in embedded systems," in *IEEE International Symposium on DFT in VLSI and Nanotechnology Systems*, pp. 228–233, IEEE, 2014.

[12] S. Venkatesha and R. Parthasarathi, "Survey on redundancy based-fault tolerance methods for processors and hardware accelerators-trends in quantum computing, heterogeneous systems and reliability," *ACM Computing Surveys*, 2024.

[13] K.-H. Huang *et al.*, "Algorithm-based fault tolerance for matrix operations," *IEEE Trans. on computers*, vol. 100, no. 6, pp. 518–528, 1984.

[14] Z. Gao, Y. Qi, J. Shi, Q. Liu, G. Ge, Y. Wang, and P. Reviriego, "Detect and replace: Efficient soft error protection of fpga-based cnn accelerators," *IEEE Transactions on Very Large Scale Integration (VLSI) Systems*, 2024.

[15] J. Jung, H. So, W. Ko, S. S. Joshi, Y. Kim, Y. Ko, A. Shrivastava, and K. Lee, "Maintaining sanity: Algorithm-based comprehensive fault tolerance for cnns," in *Proceedings of the 61st ACM/IEEE Design Automation Conference*, pp. 1–6, 2024.

[16] X. Xue *et al.*, "Exploring winograd convolution for cost-effective neural network fault tolerance," *IEEE Transactions on Very Large Scale Integration (VLSI) Systems*, 2023.

[17] K. Simonyan *et al.*, "Very deep convolutional networks for large-scale image recognition," *arXiv preprint arXiv:1409.1556*, 2014.

[18] A. Krizhevsky *et al.*, "Learning multiple layers of features from tiny images," *Technical Report*, 2009.

[19] K. He *et al.*, "Deep residual learning for image recognition," in *Proceedings of the IEEE conference on computer vision and pattern recognition*, pp. 770–778, 2016.

[20] D. Zhou *et al.*, "Deepvit: Towards deeper vision transformer," *arXiv preprint arXiv:2103.11886*, 2021.

[21] H. Touvron *et al.*, "Going deeper with image transformers," in *IEEE/CVF International Conf. on Computer Vision*, pp. 32–42, 2021.

[22] J. Deng *et al.*, "Imagenet: A large-scale hierarchical image database," in *2009 IEEE Conf. on CVPR*, pp. 248–255, 2009.

[23] M. Safarpour, T. Z. Deng, J. Massingham, L. Xun, M. Sabokrou, and O. Silvén, "Low-voltage energy efficient neural inference by leveraging fault detection techniques," in *2021 IEEE Nordic Circuits and Systems Conference (NorCAS)*, pp. 1–5, IEEE, 2021.

[24] S. Roffe and A. D. George, "Evaluation of algorithm-based fault tolerance for machine learning and computer vision under neutron radiation," in *2020 IEEE Aerospace Conference*, pp. 1–9, IEEE, 2020.

[25] U. Sharif, D. Mueller-Gritschneider, R. Stahl, and U. Schlichtmann, "Efficient software-implemented hw fault tolerance for tinyml inference in safety-critical applications," in *2023 Design, Automation & Test in Europe Conference & Exhibition (DATE)*, pp. 1–6, IEEE, 2023.

[26] S. Li, J. Huang, P. T. P. Tang, D. Khudia, J. Park, H. D. Dixit, and Z. Chen, "Efficient soft-error detection for low-precision deep learning recommendation models," in *2022 IEEE International Conference on Big Data (Big Data)*, pp. 1556–1563, IEEE, 2022.

[27] H. Zamani, Y. Liu, D. Tripathy, L. Bhuyan, and Z. Chen, "Greenmm: energy efficient gpu matrix multiplication through undervolting," in *Proceedings of the ACM International Conference on Supercomputing*, pp. 308–318, 2019.

[28] M. Liu, L. Xia, Y. Wang, and K. Chakrabarty, "Fault tolerance for rram-based matrix operations," in *2018 IEEE International Test Conference (ITC)*, pp. 1–10, IEEE, 2018.

[29] X. Xue, C. Liu, Y. Wang, B. Yang, T. Luo, L. Zhang, H. Li, and X. Li, "Soft error reliability analysis of vision transformers," *IEEE Transactions on Very Large Scale Integration (VLSI) Systems*, 2023.

[30] J. J. Zhang *et al.*, "Fault-tolerant systolic array based accelerators for deep neural network execution," *IEEE Design & Test*, vol. 36, no. 5, pp. 44–53, 2019.

[31] S. Chetlur *et al.*, "cudnn: Efficient primitives for deep learning," *arXiv preprint arXiv:1410.0759*, 2014.

[32] S.-J. Wang and others., "Algorithm-based fault tolerance for fft networks," *IEEE Transactions on Computers*, vol. 43, no. 7, pp. 849–854, 1994.

[33] X. Liang *et al.*, "Correcting soft errors online in fast fourier transform," in *Proceedings of the International Conference for High Performance Computing, Networking, Storage and Analysis*, pp. 1–12, 2017.

[34] A. Schöll *et al.*, "Efficient algorithm-based fault tolerance for sparse matrix operations," in *46th Annual IEEE/IFIP International Conf. on DSN*, pp. 251–262, IEEE, 2016.

[35] C. Peltekis, D. Filippas, and G. Dimitrakopoulos, "Error checking for sparse systolic tensor arrays," *arXiv preprint arXiv:2402.10850*, 2024.

[36] P. Wu *et al.*, "Towards practical algorithm based fault tolerance in dense linear algebra," in *25th ACM International Symposium on High-Performance Parallel and Distributed Computing*, pp. 31–42, 2016.

[37] G. Leon, J. M. Badia, J. A. Belloch, A. Lindoso, and L. Entrena, "Comparative analysis of soft-error sensitivity in lu decomposition algorithms on diverse gpus," *The Journal of Supercomputing*, pp. 1–19, 2024.

[38] J. Chen *et al.*, "Fault tolerant one-sided matrix decompositions on heterogeneous systems with gpus," in *SC18: International Conference for High Performance Computing, Networking, Storage and Analysis*, pp. 854–865, IEEE, 2018.

[39] Q. M. Nguyen *et al.*, "Coded qr decomposition," in *2020 IEEE International Symposium on Information Theory (ISIT)*, pp. 191–196, IEEE, 2020.

[40] S. Li *et al.*, "Ft-isort: Efficient fault tolerance for introsort," in *International Conf. for High Performance Computing, Networking, Storage and Analysis*, pp. 1–17, 2019.

[41] E. T. Camargo and E. P. D. Junior, "Algorithm-based fault-tolerant parallel sorting," *International Journal of Critical Computer-Based Systems*, vol. 11, no. 1-2, pp. 2–29, 2024.

[42] K. Zhao *et al.*, "Ft-cnn: Algorithm-based fault tolerance for convolutional neural networks," *IEEE Trans. on Parallel and Distributed Systems*, vol. 32, no. 7, pp. 1677–1689, 2020.

[43] J. Kosaian *et al.*, "Arithmetic-intensity-guided fault tolerance for neural network inference on GPUs," in *International Conf. for HPC, Networking, Storage and Analysis*, pp. 1–15, 2021.

[44] S. Wu *et al.*, "Anatomy of high-performance gemm with online fault tolerance on gpus," *arXiv preprint arXiv:2305.01024*, 2023.

[45] Y. Liang, X. Li, J. Ren, A. Li, B. Fang, and J. Chen, "Light-weight fault tolerant attention for large language model training," 2024.

[46] S. Wu, Y. Zhai, J. Liu, J. Huang, Z. Jian, H. Dai, S. Di, Z. Chen, and F. Cappello, "Turbofft: A high-performance fast fourier transform with fault tolerance on gpu," *arXiv preprint arXiv:2405.02520*, 2024.